Available online at www.sciencedirect.com
SCIENCE DIRECT®
Chemical Physics Letters 368 (2003) 445–451
CHEMICAL PHYSICS LETTERS
www.elsevier.com/locate/cplett

Absolute chlorine atom quantum yield measurements in the UV and VUV gas-phase laser photolysis of CCl_4

Alexander Hanf, Almuth Läuter, Hans-Robert Volpp *

Physikalisch-Chemisches Institut der Universität Heidelberg, Im Neuenheimer Feld 253, D-69120 Heidelberg, Germany

Received 16 October 2002

Abstract

Absolute quantum yields Φ_{Cl+Cl^*} for the formation of chlorine atoms were measured under collision-free conditions for the gas-phase dissociation of carbon tetrachloride (CCl_4) after pulsed laser photoexcitation at 193 and 135 nm. By means of a photolytic calibration method, where the gas-phase photolysis of HCl was utilized as a reference, values of Φ_{Cl+Cl^*} (193 nm) = 1.5 ± 0.1 and Φ_{Cl+Cl^*} (135 nm) = 1.9 ± 0.1 could be obtained which demonstrate the importance of the ultraviolet (UV) and vacuum-UV photolysis of CCl_4 as an efficient source of atomic chlorine formation.

1. Introduction

Carbon tetrachloride (CCl_4) has been widely used as an organic solvent until it has been realized that after being released to the atmosphere it can be decomposed by ultraviolet (UV) and vacuum-ultraviolet (VUV) radiations in the stratosphere leading to the formation of chlorine atoms which enter into the ozone destroying ClO_x cycle [1–3]. Among the chlorinated and fluorinated methanes involved in the stratospheric ozone destruction CCl_4 has the highest ozone depletion potential (ODP) [4]. As a consequence, much effort has gone into the determination of the optical absorption spectrum in the UV and VUV spectral regions [5–10], as well as into the measurement of nascent photoproduct fluorescence yields after excitation by VUV radiation [8,9,11,12]. In addition, studies on the formation dynamics of ground-state $Cl(^2P_{3/2})$ and spin–orbit excited $Cl^*(^2P_{1/2})$ chlorine atoms after UV and VUV laser photoexcitation were carried out [13,14]. However, as far as the primary quantum yield for chlorine atom formation is concerned, to the best of our knowledge, no direct measurements of this quantity under collision-free conditions have been reported so far.

The focus of the work to be presented in the following was on the measurement of the absolute quantum yield for chlorine atom formation in the 193 and 135 nm photolysis of CCl_4. The present experiments were performed under collision-free conditions in a low-pressure flow reactor at room temperature using the pulsed laser photolysis/vacuum-ultraviolet laser-induced fluorescence (LP/VUV-LIF) 'pump-and-probe' technique in combination with a photolytic calibration approach.

* Corresponding author. Fax: +49-(0)-6221-545-050.
E-mail address: aw2@ix.urz.uni-heidelberg.de (H.-R. Volpp).

0009-2614/02/$ - see front matter © 2002 Published by Elsevier Science B.V.
PII: S0009-2614(02)01896-1

2. Experimental

The CCl_4 gas-phase photolysis studies were carried out in a flow reactor using the experimental arrangement described in detail elsewhere [15]. Hence, only experimental details relevant to the present studies will be given in the following.

CCl_4 (AppliChem, >99%) degassed prior to use by several freeze–pump–thaw cycles was pumped through the reactor at room temperature. The gas flow rate in the reactor was set high enough to ensure fresh sample gases between successive laser shots at the laser repetition rate of 6 Hz. In the UV and VUV photolysis experiments the CCl_4 pressure was typically 10–18 mTorr. For the photolytic calibration HCl (Messer Griesheim, 99.99%) was pumped through the cell at pressures of typically 50–70 mTorr (UV photolysis) and 400-450 mTorr (VUV photolysis).

In the first part of the work the unpolarized output of an ArF excimer laser (193 nm emission wavelength, pulse duration 15–20 ns) was employed as a photolysis ('pump') laser to dissociate the CCl_4 parent molecules. Very low pump laser intensities (2–5 mJ/cm^2) had to be employed during the measurements in order to avoid multiphoton dissociation of CCl_4 (which could be observed at pump laser intensities >30 mJ/cm^2). As depicted in Fig. 1a, a linear dependence of the chlorine atom signal on the pump laser intensity was observed under the low pump laser intensity conditions of the present experiments demonstrating that the Cl and Cl* photofragments originate from a one-photon dissociation process.

For LIF detection of chlorine atoms, narrowband VUV 'probe' laser radiation ($\Delta\omega_{VUV} \approx 0.3$ cm^{-1}) tunable in the wavelength region 133.5–136.4 nm was generated by resonant third-order sum-difference frequency conversion of pulsed dye laser radiation (pulse duration 15–20 ns) in Kr [16]. In the four-wave mixing process ($\omega_{VUV} = 2\omega_R - \omega_T$) the first frequency ω_R ($\lambda_R = 212.55$ nm) is two-photon resonant with the Kr 4p–5p $(1/2, 0)$ transition and kept fixed during the measurement. The second frequency ω_T could be tuned from 480 to 521 nm to cover the four allowed $Cl(4s^2P_{j'} \leftarrow 3p^2P_{j''};\ j' = 1/2, 3/2 \leftarrow j'' = 1/2, 3/2)$ transitions [17]. Ground-state $Cl(^2P_{3/2})$ and excited-state $Cl^*(^2P_{1/2})$ atom fragments were detected employing the $(j' = j'')$-transitions at $\omega_{Cl} = 74228.0$ cm^{-1} (134.72 nm) and $\omega_{Cl^*} = 73980.9$ cm^{-1} (135.17 nm), respectively, which have the highest transition probabilities [18]. The probe laser beam was aligned to overlap the pump laser beam at right angles in the viewing region of the LIF detector. The delay time between pump and probe laser pulses was typically 150 ± 10 ns, which allowed the collision-free detection of the nascent

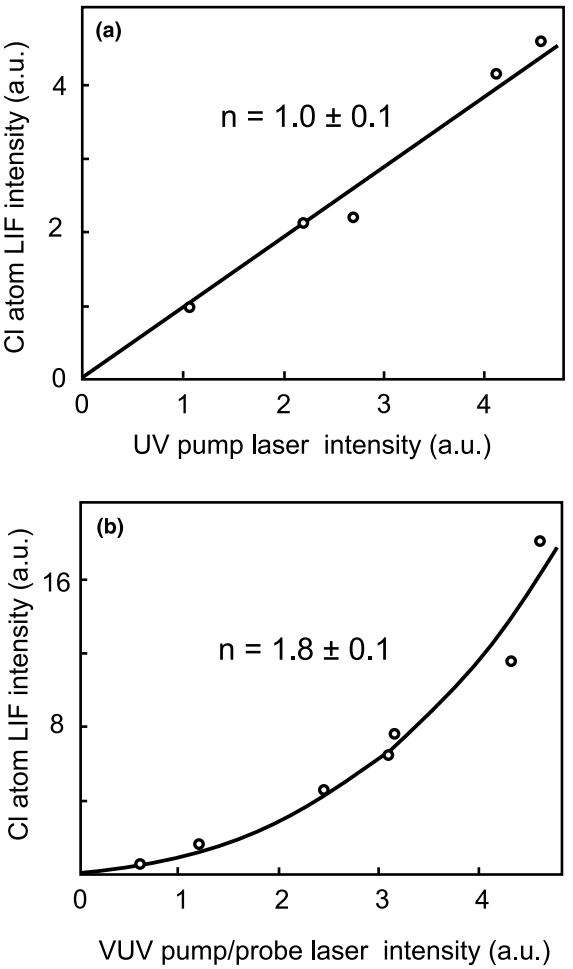

Fig. 1. Dependence of the Cl atom signal (a) on the photolysis ('pump') laser intensity in the 193 nm photolysis of CCl_4 and (b) on the VUV 'pump/probe' laser intensity as obtained in the 135 nm CCl_4 photodissociation experiments. Solid lines are the result of a least-squares fit (I^n_{pump}) to the experimental data in order to determine the power-dependence n of the respective LIF signals. The values obtained for n are given in the figure.

Cl and Cl* atom products under the low-pressure conditions of the experiments. Under the present experimental conditions, relaxation of Cl* by quenching as well as fly out of the Cl, Cl* atoms and secondary reactions with CCl_4 or HCl were negligible. In the two-color, 193 nm pump and VUV probe, photolysis experiments the 'VUV-self-photolysis-background' subtraction method used in our previous CH_3CF_2Cl (HCFC-142b) UV photolysis studies was adapted to obtain LIF signals which originate from chlorine atoms solely produced by the 193 nm pump laser pulse (see e.g. [19]).

In the second part of the study, the VUV laser radiation was utilized to photodissociate the CCl_4 parent molecules as well as to detect the nascent Cl, Cl* photodissociation products within the same laser pulse (the duration of the laser pulse was about 10–15 ns). In all experiments special care was taken to separate the VUV laser radiation from the unconverted fundamental laser beams by means of a lens monochromator (see Fig. 1 of [20]). Cl and Cl* LIF signals were observed through a band pass filter, ARC model 130-B-1D, by a solar blind photomultiplier positioned at right angles to both pump and probe laser. During the measurements the VUV laser beam intensity was monitored with an additional solar blind photomultiplier. Each point of the recorded Cl, Cl* atom Doppler profiles was averaged over 30 laser shots at a laser repetition rate of 6 Hz. LIF signals, UV pump and VUV probe beam intensities were recorded with a boxcar integrator system.

In the two-color (193 nm pump and VUV probe) experiments care was taken that the observed Cl, Cl* atom LIF signals in the CCl_4 (see Fig. 1a) as well as in the HCl photolysis showed a linear dependence on the pump laser and on the VUV probe laser intensities. In these experiments the Cl, Cl* atom LIF signals were normalized point-by-point to the UV pump and VUV probe laser intensity.

In the one-color (VUV pump–probe) experiments the Cl, Cl* atom LIF signals were normalized point-by-point to the square of the VUV (pump/probe) laser intensity. The $(n = 1 + 1)$-photon nature – one-photon parent CCl_4 molecule dissociation followed by a one-photon Cl, Cl* atom LIF-detection step – of the process was experimentally verified by varying the VUV laser intensity (see Fig. 1b). Similar measurements were performed in case of HCl where a value of $n = 2.0 \pm 0.1$ was obtained. From the observed VUV laser intensity dependence it can be concluded that 'secondary' photolysis of photodissociation products can be neglected.

3. Results

Absolute primary quantum yields Φ_{Cl} (193 nm) for Cl and Φ_{Cl^*} (193 nm) for Cl* atom formation were determined in separate measurements by calibrating the Cl, Cl* atom signals $S_{Cl}(CCl_4), S_{Cl^*}(CCl_4)$ observed in the 193 nm photodissociation of CCl_4 against the Cl, Cl* atom signals $S_{Cl}(HCl)$, $S_{Cl^*}(HCl)$ of the well-defined Cl, Cl* atom number densities generated in the 193 nm photolysis of HCl (see Fig. 2). Values for Φ_{Cl} (193 nm) and Φ_{Cl^*} (193 nm) were derived via Eqs. (1a) and (1b), respectively, [19]

$$\Phi_{Cl}\ (193\ \text{nm}) = \gamma_{Cl}\{S_{Cl}(CCl_4)\phi_{Cl}\sigma_{HCl}p_{HCl}\} / \{S_{Cl}(HCl)\sigma_{CCl_4}p_{CCl_4}\}, \quad (1a)$$

$$\Phi_{Cl^*}\ (193\ \text{nm}) = \gamma_{Cl^*}\{S_{Cl^*}(CCl_4)\phi_{Cl^*}\sigma_{HCl}p_{HCl}\} / \{S_{Cl^*}(HCl)\sigma_{CCl_4}p_{CCl_4}\}, \quad (1b)$$

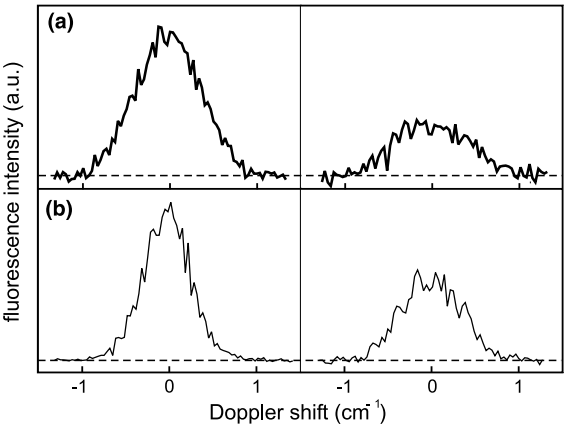

Fig. 2. Cl and Cl* atomDoppler profiles measured in the 193 nm photolysis of (a) 14 mTorr of CCl_4 and (b) 70 mTorr of HCl.

where σ_{HCl} and σ_{CCl_4} are the room-temperature optical absorption cross-sections of HCl and CCl_4 at the photodissociation wavelength 193 nm. S_{Cl} and S_{Cl^*} are the integrated areas under the measured Cl and Cl^* atom Doppler profiles and p_{HCl} and p_{CCl_4} are the pressures of HCl and CCl_4, respectively. $\phi_{Cl^*}(193\ nm) = 0.40$ and ϕ_{Cl} (193 nm) = 0.60 are the Cl and Cl^* atom quantum yields in the 193 nm photolysis of HCl, which can be derived from the $[Cl^*]/[Cl]$ spin–orbit branching ratio, 0.67 ± 0.09, obtained previously [19]. For the HCl absorption cross-sections, the value $\sigma_{HCl} = (8.1 \pm 0.4) \times 10^{-20}$ cm^2 was used, which has been measured for the ArF excimer laser emission wavelength (193 nm) [21]. For the CCl_4 absorption cross-section the value $\sigma_{CCl_4} = (8.6 \pm 0.5) \times 10^{-19}$ cm^2 was used which was measured in the course of the present work. The latter value is in good agreement with the value $\sigma_{CCl_4} = 8.4 \times 10^{-19}$ cm^2 which can be derived from the absorption cross-section data reproduced in [22].

In Eqs. (1a) and (1b), the factors γ_{Cl^*} and γ_{Cl} are corrections accounting for the different degrees of absorption of the VUV probe laser radiation by CCl_4 and HCl. These correction factors could be directly determined from the known distances inside the flow cell and the relative difference in the probe laser attenuation measured in the CCl_4 and HCl photolysis runs. Under the present experimental conditions the absorption corrections were $\gamma_{Cl} \approx \gamma_{Cl^*} = 0.75 \pm 0.03$. The experimental data sets which were evaluated via Eqs. (1a) and (1b) to determine Φ_{Cl} (193 nm) and Φ_{Cl^*} (193 nm) consisted of 19 Cl (Cl^*) atom profiles obtained in combination with 19 Cl (Cl^*) profiles from HCl calibration runs. Experimental errors were determined from the 1σ statistical uncertainties of the experimental data, the uncertainties of the CCl_4 and HCl optical absorption cross-sections and the uncertainty of the $[Cl^*]/[Cl]$ value in the 193 nm photolysis of HCl using simple error propagation. Values of Φ_{Cl} (193 nm) $= 1.1 \pm 0.05$ and Φ_{Cl^*} (193 nm) $= 0.4 \pm 0.02$ were obtained from which a value of Φ_{Cl+Cl^*} (193 nm) $= 1.5 \pm 0.1$ can be derived for the total chlorine atom quantum yield in the 193 nm photolysis of CCl_4.

In a similar way absolute primary quantum yields Φ_{Cl} (135 nm) and Φ_{Cl^*} (135 nm) were determined for the 135 nm VUV photodissociation of CCl_4 (see Fig. 3). In this case values of ϕ_{Cl^*} (135 nm) = 0.36 and ϕ_{Cl} (135 nm) = 0.64 for the Cl and Cl^* quantum yields in the 135 nm photolysis of HCl were used in the evaluation, which could be derived from the spin–orbit branching ratio, $[Cl^*]/[Cl] = 0.56 \pm 0.03$ measured in the present work. The latter value of the chlorine atom spin-orbit branching ratio is in very good agreement with theoretical results of quantum mechanical scattering calculations of the HCl photodissociation dynamics [23]. Absorption cross section values of $\sigma_{HCl} = (1.1 \pm 0.1) \times 10^{-18}$cm^2 and $\sigma_{CCl_4} = (6.3 \pm 0.5) \times 10^{-17}$ cm^2, obtained in the course of the present work, were used in the data evaluation of the 135 nm photolysis experiments. Both values agree, within the combined error limits, with the corresponding values of $\sigma_{HCl} = (1.2 \pm 0.1) \times 10^{-18}$ cm^2 and $\sigma_{CCl_4} = (5.6 \pm 0.6) \times 10^{-17}$ cm^2, which can be derived from the absorption cross-section data reproduced in [24] and [9], respectively. For the pressure conditions of the 135 nm quantum yield measurements the correction factors were $\gamma_{Cl} \approx \gamma_{Cl^*} = 0.95 \pm 0.04$. Evaluation of 10 Cl ($Cl^*$) atom profiles obtained in combination with 10 Cl (Cl^*) profiles from HCl calibration runs yielded values of Φ_{Cl} (135 nm) $= 1.5 \pm 0.07$ and Φ_{Cl^*} (135 nm) $= 0.4 \pm 0.02$ which result in a value of Φ_{Cl+Cl^*}

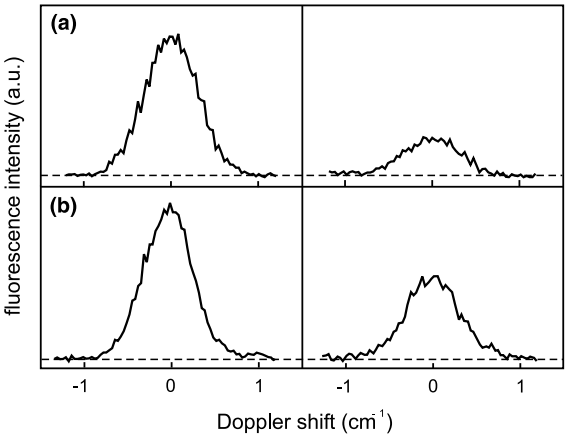

Fig. 3. Cl and Cl^* atomDoppler profiles measured in the 135 nm photolysis of (a) 18 mTorr of CCl_4 and (b) 450 mTorr of HCl.

(135 nm) = 1.9 ± 0.1 for the total chlorine atom quantum yield in the 135 nm photolysis of CCl_4.

4. Discussion

The observation of primary chlorine atom product quantum yields Φ_{Cl+Cl^*} (193 nm) = 1.5 ± 0.1 and Φ_{Cl+Cl^*} (135 nm) = 1.9 ± 0.1, which are considerably higher than unity, is consistent with the fact that for both photolysis wavelengths the corresponding photon energies, $\hbar\omega$ (193 nm) = 6.4 eV and $\hbar\omega$(135nm) = 9.2 eV, are high enough to break two C–Cl bonds [11].

For the 193 nm photolysis wavelength, which leads to an excitation in the red edge of the first absorption band of CCl_4, denoted as A($1t_1$–σ^*) valence band in [9], chlorine atoms can be only formed via two dissociation pathways (all dissociation energies E_d given in the following were taken from Table 1 of [11] and refer to the Cl atom formation channel)

$$CCl_4(\tilde{X}^1A_1) + \hbar\omega \rightarrow CCl_3(\tilde{X}^2A_1) + Cl(Cl^*)$$
$$E_d = 2.94 \text{ eV}, \quad (2)$$

$$CCl_4(\tilde{X}^1A_1) + \hbar\omega \rightarrow CCl_2(\tilde{X}^1A_1) + 2Cl(Cl^*)$$
$$E_d = 5.91 \text{ eV}. \quad (3)$$

Therefore, the present result of Φ_{Cl+Cl^*} (193 nm) = 1.5 ± 0.1 implies that substantial amounts of the observed chlorine atoms must be formed via the three-body decay channel (3) along with $CCl_2(\tilde{X}^1A_1)$ products. The latter implication is consistent with the results of previous photodecomposition studies at 214 and 185 nm in which primary quantum yields for CCl_3 and CCl_2 formation were determined from the analysis of stable photochemical reaction products after irradiation of static CCl_4 samples in the presence of different radical scavenging agents [25,26]. These studies revealed a pronounced increase in the CCl_2 quantum yield after the photolysis wavelength was decreased from 214 to 185 nm. In addition, these studies along with the results obtained at a photolysis wavelength of 163 nm [26] (which leads to an excitation in the blue edge of the A band) indicate that at the same time the CCl_3 quantum yield decreases rapidly with decreasing photolysis wavelength (see Table 1).

At a shorter photolysis wavelength of 147 nm, which results in B($1t_1$–4s) band Rydberg excitation of CCl_4 [9], the rather low CCl_3 quantum yield $\Phi_{CCl_3} = 0.04 \pm 0.02$ determined in [26] demonstrates that the C–Cl single-bond cleavage pathway (2) is only of minor importance in the VUV photolysis of CCl_4. The low value of the CCl_3 quantum yield along with the CCl_2 quantum yield of $\Phi_{CCl_2} = 0.6 \pm 0.2$ led the authors of [26] to the conclusion that an additional three-body fragmentation process of the kind

$$CCl_4(\tilde{X}^1A_1) + \hbar\omega \rightarrow CCl(X^2\Pi) + Cl_2 + Cl(Cl^*)$$
$$E_d = 7.38 \text{ eV}, \quad (4)$$

Table 1
Quantum yields of primary products formed in the gas-phase photolysis of CCl_4 at different UV and VUV photodissociation wavelengths λ_{photo}

λ_{photo}	254 (4.9)	214 (5.8)	193 (6.4)	185 (6.7)	163 (7.6)	147 (8.4)	135 (9.2)
Φ_{CCl_3}		0.9 ± 0.1[b]		0.4[c]	0.25 ± 0.05[b]	0.04 ± 0.02[b]	
Φ_{CCl_2}		0.05 ± 0.03[b]		0.6[c]	0.76 ± 0.2[b]	0.6 ± 0.2[b]	
Φ_{CCl}						0.36 ± 0.22[d]	
Φ_{Cl+Cl^*}	0.9 ± 0.1[a]	1.0 ± 0.13[f]	1.5 ± 0.1[e]	1.6[f]	1.77 ± 0.3[f]	1.6 ± 0.64[f]	1.9 ± 0.1[e]

λ_{photo} is given in nm. The corresponding excitation energies $\hbar\omega_{photo}$ are given in parentheses in units of eV.
[a] From [25] (derived from Br_2 consumption measurements in the 254 nm photolysis of CCl_4/Br_2 mixtures).
[b] From [26].
[c] Values reported in [25].
[d] Value calculated from the respective values of Φ_{CCl_3} and Φ_{CCl_2} : $\Phi_{CCl} = 1 - \Phi_{CCl_3} - \Phi_{CCl_2}$.
[e] Present work.
[f] Values calculated from the respective values of Φ_{CCl_3}, Φ_{CCl_2} and Φ_{CCl} : $\Phi_{Cl+Cl^*} = \Phi_{CCl_3} + 2 \times \Phi_{CCl_2} + \Phi_{CCl}$ (for details see text).

which does not result in CCl_3 or CCl_2 formation must be operating at that wavelength. CCl radical formation was already proposed in [25] in conjunction with the results of previous 147 nm photodecomposition studies of CCl_4. Following this proposition, a CCl quantum yield of 0.36 (see Table 1) can be derived from the given values of Φ_{CCl_3} and Φ_{CCl_2} via $\Phi_{CCl} = 1 - \Phi_{CCl_3} - \Phi_{CCl_2}$ (in this calculation a total CCl_4 photodestruction yield of unity was assumed which is not unreasonable considering the absence of any vibrational structure in the B absorption band of CCl_4 [9]). As can be seen in Fig. 4, the resulting chlorine atom quantum yield Φ_{Cl+Cl^*} (147 nm) $= 1.6 \pm 0.64$ is not inconsistent with the chlorine atom quantum yields derived from the UV (A band) photolysis studies and the chlorine atom yield measured in the present work at 135 nm (see also Table 1).

The 135 nm photolysis wavelength excites CCl_4 in the red edge of the first component of the strong X band doublet of the absorption spectrum, which has been assigned to a ($2t_2$–4s) Rydberg transition

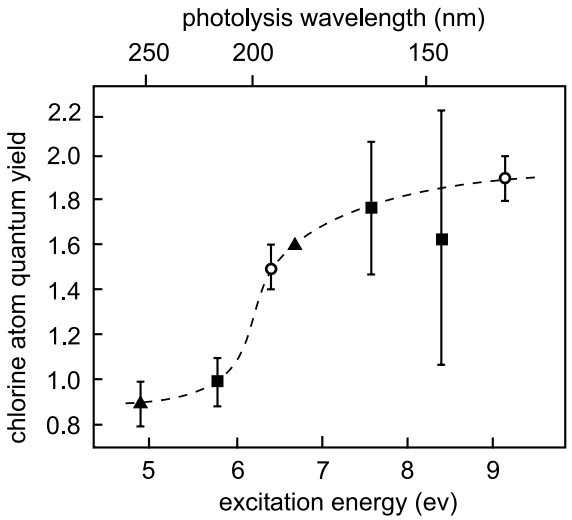

Fig. 4. Primary quantum yields for chlorine atom formation (Φ_{Cl+Cl^*}) in the UV and VUV photolysis of CCl_4. Values are plotted against excitation energy. Open circles are the results of the present direct measurements. Solid symbols represent values derived from the analysis of stable photochemical reaction products observed after the irradiation of static CCl_4 samples [25,26]. For further details see text and Table 1. The dashed line is included just to guide the eyes.

[9]. The observation of $CCl_2(\tilde{A}^1B_1–\tilde{X}^1A_1)$ fluorescence emission which closely follows the shape of the D($1t_1$–4p) and X($2t_2$–4s; $2t_2$–4p) band absorption spectrum in the 140–120 nm wavelength region indicates that for photolysis wavelengths <150 nm a new chlorine atom formation channel (5) which results in electronically excited CCl_2 fragments starts to operate [11]

$$ClCl_4(\tilde{X}^1A_1) + \hbar\omega \rightarrow CCl_2(\tilde{A}^1B_1) + 2Cl(Cl^*)$$
$$E_d = 8.05 \text{ eV}. \quad (5)$$

Although this reaction channel might not contribute significantly to chlorine atom production in the 147 nm photolysis (as indicated by the quite small $CCl_2(\tilde{A}^1B_1–\tilde{X}^1A_1)$ fluorescence cross-section observed across the B band) a substantial contribution to the chlorine atom formation can be inferred for the 135 nm photolysis wavelength from the pronounced increase in the subsequent D and X bands (see e.g. Fig. 1 in [9]).

5. Summary

Absolute quantum yields for the formation of chlorine atoms Φ_{Cl+Cl^*} (193 nm) $= 1.5 \pm 0.1$ and Φ_{Cl+Cl^*} (135 nm) $= 1.9 \pm 0.1$ were measured in gas-phase photodissociation studies of CCl_4 under collision-free conditions. The fact that both values are considerably higher than unity demonstrates the presence of chlorine atom producing three-body decay channels, which emphasize the importance of the UV and VUV photolysis of CCl_4 as a quite efficient source of atomic chlorine in the earth's atmospheric photochemistry.

Acknowledgements

Partial financial support by the Deutsche Forschungsgemeinschaft (DFG) is gratefully acknowledged. AL was supported by the Landesgraduierten Förderung Baden-Württemberg. We thank Dhanya Suresh for her help in the VUV photolysis experiments. HRV wants to thank Prof. J. Wolfrum (Director of the Institute of Physical Chemistry, Ruprecht-Karls-University Heidelberg) for his continuous interest in the present work.

References

[1] P.J. Crutzen, in: B.M. McCormac (Ed.), Physics and Chemistry of Upper Atmospheres, Reidel, Dordrecht, 1973.
[2] M.J. Molina, F.S. Rowland, Nature 249 (1974) 810.
[3] R. Zellner (Ed.), Global Aspects of Atmospheric Chemistry, Springer, Heidelberg, 1999.
[4] R.P. Wayne, Chemistry of Atmospheres, Oxford University, Oxford, 1991.
[5] H. Tsubomura, K. Kimura, K. Kaya, J. Tanaka, S. Nagakura, Bull. Chem. Soc. Jpn. 37 (1964) 417.
[6] B.R. Russel, L.O. Edwards, J.W. Raymonda, J. Am. Chem. Soc. 95 (1973) 2129.
[7] G.C. Causely, B.R. Russel, J. Electron Spectrosc. Relat. Phenom. 11 (1977) 383.
[8] T. Ibuki, N. Takahashi, A. Hiraya, K. Shobatake, J. Chem. Phys. 85 (1986) 5717.
[9] L.C. Lee, M. Suto, Chem. Phys. 114 (1987) 423.
[10] G.H. Ho, Chem. Phys. 226 (1998) 101.
[11] H. Biehl, K.J. Boyle, D.P. Seccombe, D.M. Smith, R.P. Tuckett, H. Baumgärtel, H.W. Jochims, J. Electron Spectrosc. Relat. Phenom. 97 (1998) 89, and references therein.
[12] Y. Hatano, Phys. Rep. 313 (1999) 109.
[13] K. Tonokura, Y. Mo, Y. Matsumi, M. Kawasaki, J. Phys. Chem. 96 (1992) 6688, and references therein.
[14] Y. Matsumi, K. Tonokura, M. Kawasaki, T. Ibuki, J. Chem. Phys. 97 (1992) 5261.
[15] R.A. Brownsword, M. Hillenkamp, T. Laurent, R.K. Vatsa, H.-R. Volpp, J. Chem. Phys. 106 (1997) 4436.
[16] G. Hilbert, A. Lago, R. Wallenstein, J. Opt. Soc. Am. B 4 (1987) 1753.
[17] K. Tonokura, Y. Matsumi, M. Kawasaki, S. Tasaki, R. Bersohn, J. Chem. Phys. 97 (1992) 8210, and references therein.
[18] W.L. Wiese, M.W. Smith, B.M. Miles, Atomic Transition Probabilities, Natl. Bur. Stand. Ref. Data Ser., Natl. Bur. Stand. (U.S.) Circ. No 22, U.S. GPO, Washington, DC, 1969.
[19] R.A. Brownsword, P. Schmiechen, H.-R. Volpp, H.P. Upadhyaya, Y.J. Jung, K.-H. Jung, J. Chem. Phys. 110 (1999) 11823.
[20] R.A. Brownsword, M. Hillenkamp, T. Laurent, R.K. Vatsa, H.-R. Volpp, J. Chem. Phys. 106 (1997) 1359.
[21] Y. Mo, K. Tonokura, Y. Matsumi, M. Kawasaki, T. Sato, T. Arikawa, P.T.A. Reilly, Y. Xie, Y. Yag, Y. Huag, R.J. Gordon, J. Chem. Phys. 97 (1992) 4815.
[22] F.S. Rowland, M.J. Molina, Rev. Geophys. Space Phys. 13 (1975) 1.
[23] H.M. Lambert, P.J. Dagdigian, M.H. Alexander, J. Chem. Phys. 108 (1998) 4460.
[24] J.B. Nee, M. Suto, L.C. Lee, J. Chem. Phys. 85 (1986) 719.
[25] D.D. Davis, J.F. Schmidt, C.M. Neeley, R.J. Hanrahan, J. Phys. Chem. 79 (1975) 11.
[26] R.E. Rebbert, P.J. Ausloos, J. Photochem. 6 (1976/1977) 265.